Nanoscale

Accepted Manuscript

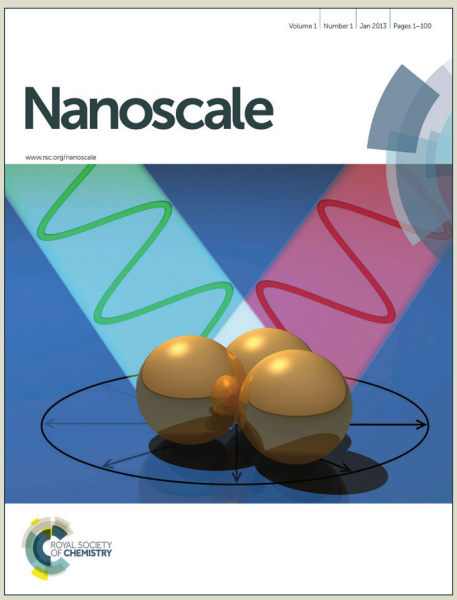

ROYAL SOCIETY OF CHEMISTRY

www.rsc.org/nanoscale

Nanoscale

PAPER

Combination of Carbon Dot and Polymer Dot Phosphors for White Light-Emitting Diodes

Received 00th January 20xx,
Accepted 00th January 20xx

DOI: 10.1039/x0xx00000x

www.rsc.org/

Chun Sun[a], Yu Zhang[a,b,c,*], Kai Sun[a], Claas Reckmeier[b], Tieqiang Zhang[c], Xiaoyu Zhang[a], Jun Zhao[d], Changfeng Wu[a,*], William W. Yu[a,d] and Andrey L. Rogach[b]

We realized white light-emitting diodes with high color rendering index (85 – 96) and widely variable color temperatures (2805 – 7786 K) by combining three phosphors based on carbon dots and polymer dots, whose solid-state photoluminescence self-quenching was efficiently suppressed within a polyvinyl pyrrolidone matrix.All three phosphors exhibited dominant absorption in UV spectral region, which ensured the weak reabsorption and no energy transfer crosstalk. The WLEDs showed excellent color stability against the increasing current because the similar response of the tricolor phosphors to the UV light variation.

1.Introduction

Solid-state white light-emitting diodes (WLEDs) are promising illumination sources to replace traditional incandescent bulbs, owing to their projected long working life time, low power consumption, fast response time, and compact size.[1-5] Currently, one common production route towards WLEDs is to combine blue-emitting LED chips with broadband yellow-emitting color converter phosphors, such as YAG:Ce^{3+},[6] Ba_3SiO_5:Eu^{2+},[7] and Sr_3SiO_5.[8,9] However, this type of WLEDs typically has relatively weak emission in the red spectral region.[10] In addition, the electroluminescence (EL) intensity of the blue light from LED chip increases much faster than that of the yellow band from the phosphors at higher currents, and the spectral position of the blue band may also change with working current. These issues result in high correlated color temperature (CCT) and low color rendering index (CRI) for these blue-yellow LEDs.[11] It is therefore highly desirable to acquire the white-light emission independent of the input power, especially when the WLEDs are used as the backlight for displays.[12,13] In the attempt to solve this issue, WLEDs employing ultraviolet (UV) LED chips as the excitation source have been explored, due to the prospects of chromatic flexibility, stability and high efficiency.[14-17] The UV chips emit light with the wavelength shorter than 400 nm, which itself has little effect on the chromaticity coordinates of the WLEDs.[11,14] Thus, the use of single or multicolor phosphors excited by UV chips has been regarded as a promising design for WLED fabrication.[18] Although single phosphors combined with UV LEDs can be fabricated easily, their CCT cannot be readily varied while maintaining the high CRI.[19,20] Coating UV LEDs with multicolor phosphors can maintain high CRI through changing the ratio of the phosphors.[21] However, small Stokes shift among these phosphors often results in a strong reabsorption of emitted light, which may cause both color instability and the decrease of the luminous efficiency.[18,22,23] Thus, combinations of phosphors which absorb only UV light but emit different colors of the visible light are highly desirable to achieve stable and efficient WLEDs.

Recently, carbon dots (CDs) have been identified as an attractive class of phosphors.[24] They show strong absorption in the near UV spectral region and the efficient blue light emission (up to 80% quantum yield (QY) for solution-based particles[25-27]), and are considered to be low toxic materials,[28-32] which make them suitable as a blue-emitting component for WLEDs.[21,33-36] However, the solid-state PL performance of CDs is still not satisfactory, largely because of the luminescence quenching due to the aggregation of CDs.[26,37] The aggregation issue could be avoided by dispersing CDs in silicone,[10,34] PMMA[21] or other inert matrices. Shen's group[37] integrated water soluble CDs with starch, while Wang *et al*.[38] embedded CDs into oligomeric silsesquioxane based solid-state matrix and combined them with NaCl protected CdTe quantum dots (QDs) to realize white-light solid state emitters. However, II-VI QDs have intrinsically small Stokes shifts, thus suffering from the emission self-quenching in solid state.[22]

To overcome these drawbacks, we have combined blue-emitting CDs with green- and red-emitting polymer dots (PDs) with large Stokes shifts. By dispersing the CDs and PDs in a highly transparent polyvinyl pyrrolidone (PVP) matrix, solid state downconversion WLEDs excited by UV chips were fabricated. They possessed high CRI and adjustable CCT, and

[a] State Key Laboratory on Integrated Optoelectronics, and College of Electronic Science and Engineering, Jilin University, Changchun 130012, China E-mail: yuzhang@jlu.edu.cn (Y. Zhang); cwu@jlu.edu.cn (C. Wu)
[b] Department of Physics and Materials Science and Centre for Functional Photonics (CFP), City University of Hong Kong, Hong Kong SAR
[c] State Key Laboratory of Superhard Materials, and College of Physics, Jilin University, Changchun 130012, China
[d] Department of Chemistry and Physics, Louisiana State University, Shreveport, LA 71115, USA

exhibited excellent color stability against the working current because the tricolor phosphors exhibited nearly the same response to the UV excitation and showed no saturation towards UV light.

2.Experimental Section

2.1Materials

Poly[(9,9-dioctylfluorenyl-2,7-diyl)-co-(1,4-benzo-1-thiadiazole)] (PF10BT, Mw = 15 000–200 000) was purchased from ADS Dyes (Quebec, Canada). Poly[(9,9-dioctylfluorene)-co-(4,7-di-2-thienyl-2,1,3-benzothiadiazole)] (PFTBT, Mw ≈ 37 500) was synthesized according to the previous reports.[39,40] Poly(styrene-co-maleic anhydride) (PSMA, Mw ≈ 1700, styrene content 68%), anhydrous tetrahydrofuran (THF, 99.9%) and ethylenediamine were purchased from Sigma-Aldrich. Citric acid monohydrate and polyvinyl pyrrolidone K30 (PVP, Mw ≈ 40 000) were purchased from Beijing Chemical Reagent Company. Polydimethylsiloxane (PDMS) was purchased from Dow Corning. All chemicals were used directly without further purification.

2.2Preparation of CDs

CDs were prepared according to the previous report[26] with minor modifications. In a typical synthesis, citric acid monohydrate (1.0507 g), ethylenediamine (335 μL) and deionized water (10 mL) were sealed into a Teflon-lined autoclave (30 mL) and heated at 200 ºC for 5 h. After the reaction, the autoclave was cooled to room temperature, and the solution was filtered using a 0.22 μm filter to remove large aggregates. The product was purified by dialysis against double-distilled water using a dialysis membrane (1000 Da, molecular weight cut-off) for 24 h. Finally, a clear yellow−brown aqueous dispersion containing CDs was obtained.

2.3 Preparation of PDs

PDs were prepared by a modified precipitation method.[40,41] In a typical synthesis, a THF solution (5 mL) of PFTBT or PF10BT (500 ppm) and PSMA (10 ppm) was sonicated to form a homogeneous mixture. The solution was injected quickly into deionized water (10 mL) in a bath sonicator. The THF was removed and the solution was concentrated under a stream of nitrogen gas on a 90°C hotplate. The solution was cooled to room temperature, and filtered through a 0.22 μm filter to remove large aggregates.

2.4 Preparation of CD/PVP and PD/PVP phosphors

CDs (0.156 mg/mL, 6 mL) or PDs (PF10BT, 0.028 mg/mL, or PFTBT, 0.06 mg/mL) and PVP (0.7g) were mixed in water under ultrasonic treatment for 2 h and the mixtures were dried in an oven at 80°C for 12 h. Dried blocks were subjected to grinding in agate mortar and screening out by mesh sieve to obtain finely dispersed CD/PVP and PD/PVP powders.

2.5 Fabrication of WLEDs

UV LED chips (LUMEX-SSL-LXTO46UV1C) with the peak emission wavelength centered at 385 nm were used for the fabrication of WLEDs. A certain amount of CD/PVP and PD/PVP were dispersed in hexane and 1 mL of silicone was added into the mixture. The mixture was vibrated for 20 min, subjected to vacuum for 1 h, coated onto the UV LED chips and cured at 80°C for 2 h.

2.6 Characterization

The nanoparticle size was estimated by dynamic light scattering (DLS, ZS90, Malvern). Fluorescence spectroscopy was performed with an Edinburgh Instrument FLS920P fluorescence spectrometer. The absolute PL QYs were measured by the same spectrometer using an integrating sphere with its inner face coated with BENFLEC®. UV-Vis absorption spectra were measured on a Shimadzu 3600 UV-Vis spectrophotometer. Time-resolved PL lifetime measurements were performed using a time-correlated single-photon counting (TCSPC) lifetime spectroscopy system with a picosecond pulsed diode laser (EPL-405 nm) as the single wavelength excitation light source. Transmission electron microscope (TEM) TECNAI F20 was employed to obtain images for the investigation of the morphology of the CDs and PDs. The emission spectra of the WLEDs were determined by a Zolix Omni-λ300 Monochromator/Spectrograph.

3.Results and discussion

The blue luminescent CDs were prepared following the established process with the starting materials of citric acid and ethylenediamine (Fig. S1a). The size of CDs was determined by DLS (Fig. 1a), and their average diameter was estimated as 0.9 nm. The size of CDs was also estimated by high-resolution transmission electron microscopy (HRTEM, Fig. S2), which showed that the particle size ranged from 0.8 to 2.2 nm. The absorption spectrum of CDs, presented in Fig. 1d, shows the main bands centered at 240 nm and 344 nm, with a tail extending to 500 nm. According to previous studies,[26] the peak at 344 nm with a tail extending to 500 nm corresponds to surface states, while the peak at 240 nm – to the carbonic core. Under the excitation of 380 nm, these CDs emitted strong blue light centered at 470 nm (full width at half maximum (FWHM) of 100 nm) with solution PL QY of 60%, as shown in Figs. 1e and 1f.

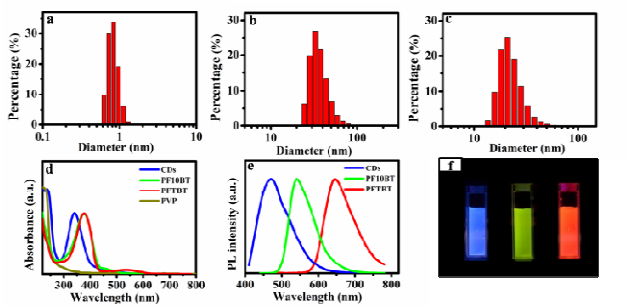

FIG. 1. Particle size histograms of CDs **(a)**, PF10BT PDs **(b)** and PFTBT PDs **(c)** determined by DLS; **(d)** UV–Vis absorption spectra of CDs, PDs, and PVP; **(e)** PL spectra of CDs and PDs; **(f)** photographs of CD and PD solutions under UV light.

The PL was significantly quenched when CDs were densely deposited on glass or plastic substrates, which is attributed to the re-absorption of emitted light. In order to prevent the PL quenching, we embedded these water-soluble CDs within a highly transparent polymer matrix of PVP to produce solid-state CD-based blue phosphors. The blue-emitting CD/PVP phosphors showed a strong PL QY of 45% in the solid state (Fig. 2a), where the shade of blue color could be varied by controlling CD loading concentration. The UV absorption spectrum of the PVP is shown in Fig. 1d. The PVP powder has almost no absorption between 340 and 600 nm where the major absorption and emission bands of CDs are located, so that the PVP matrix absorbs neither excitation light for CDs nor the emission from CDs. Water-soluble CDs have both hydroxyl and amide groups on the surface,[26] which can form hydrogen bonds with the lactam groups on PVP molecules (Fig. S5), which ensures dispersion of CDs within the PVP network, thus preventing their agglomeration and PL quenching. The absorption and PL emission spectra of the CD/PVP film are shown in Fig. S6. The peak positions were nearly the same as for the CD solution (Fig. 1d), which demonstrated that there was no change of chemical structure as a result of interaction between CDs and PVP molecules. Compared to the PL emission peak of the CD solution, no obvious shift has been observed for the CD/PVP film, while the FWHM of the CD/PVP film was 7 nm narrower than that of CD solution, which may be attributed to the influence of PVP molecules.[38,42]

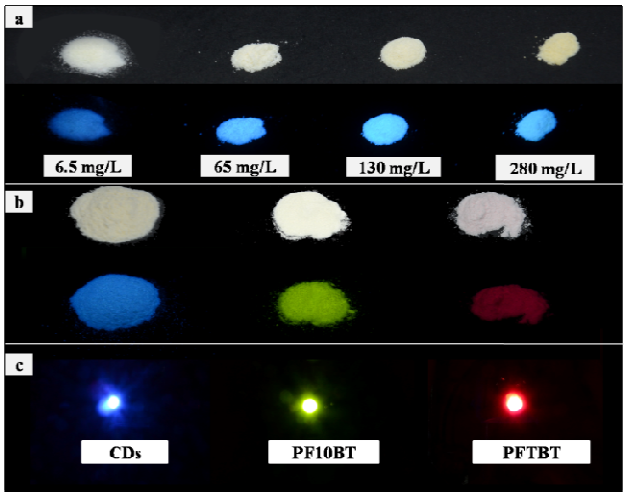

FIG. 2. (a) Photographs of CD/PVP powder phosphors with different CD concentration under daylight and UV light; **(b)** photographs of CD/PVP, PF10BT/PVP and PFTBT/PVP powder phosphors under daylight and UV light; **(c)** photographs of monochrome downconversion LEDs fabricated from CD/PVP, PF10BT/PVP and PFTBT/PVP phosphors deposited on UV chips.

In order to produce WLEDs with high color stability, green- and red-emitting conjugated PF10BT and PFTBT PDs with enlarged Stokes shift were chosen as other non-toxic light-emitting components. The enlarged Stokes shift is caused by the energy transfer from the fluorine segment to 1,4-benzo-1-thiadiazole (BT) or 4,7-di-2-thienyl-2,1,3-benzothiadiazole (DTBT), which is of great benefit to eliminate the self-absorption between these light-emitting species.[39] As presented in Figs. 1b and 1c, the average particle sizes of PF10BT and PFTBT PDs were 23 and 33 nm, respectively. The size of both kind of PDs were also characterized by TEM (Fig. S3 and S4), which demonstrated that the PDs exhibited spherical shape with uniform dispersion. As TEM shows, the average particle sizes of PF10BT and PFTBT PDs were 22 and 32 nm, respectively, which is consistent with the DLS data. Both of them exhibited the dominant UV absorption band at 375 nm corresponding to fluorene segments, with negligible tails at 450 nm and 520 nm representing the BT and DTBT segments incorporated into the polyfluorene main chain,[39] so that both PDs can be simultaneously excited by UV light. As Fig. 1e and 1f show, PF10BT and PFTBT PDs emitted green and red light with PL centered at 541 nm and 645 nm, respectively. The FWHM of PDs was broad (78 nm for PF10BT and 92 nm for PFTBT), which was beneficial for the fabrication of high CRI WLEDs. The solution PL QYs of these green and red emitting PDs were 66% and 33%, respectively. Solid state PD/PVP phosphors were fabricated using the similar procedure as for CD/PVP (Fig. S5), and showed strong emission with the PL QYs of 60% and 30% under UV light excitation, respectively (Fig. 2b). The absorption and PL emission spectra of the PD/PVP films are shown in Fig. S6. Compared to the absorption and the PL

emission peak of the respective PD solutions, no shifts were observed for the PD/PVP films. We then fabricated monochrome blue, green and red downconversion LEDs by depositing CD/PVP and PD/PVP phosphors on UV chips (Fig. 2c).

To fabricate the WLEDs, a mixture of the blue-emitting CD/PVP and the green- and red-emitting PD/PVP were uniformly dispersed in silicone and deposited on UV chips (Fig. S5). All these tricolor phosphors exhibited broader FWHM than traditional rare-earth phosphors and semiconductor QDs, leading to substantial spectra overlap among their emission, which is beneficial for high CRI and high efficiency when fabricating WLEDs.[16,38] By varying the mass ratio of these three solid-state phosphors, the EL emission spectra of WLEDs could be adjusted towards the intensity ratio of three major peaks, as shown in Fig. 3a and Table 1. In order to distinguish component contributions into the broad EL emission spectra, we performed Gaussian fits of the experimental data as shown in Fig. S7. The simulated EL spectra showed three distinct emission peaks which were almost identical to those of CDs and PDs in solution (dashed lines in Fig. S7). For all the six fabricated WLED devices A-F, the amount of the green component was constant, and the emission spectra could be tuned by adjusting the amounts of the blue and red components. The white emission became colder with the increasing of blue component and decreasing of red component, and turned warmer if otherwise.

Table 1 shows the characteristics of the six fabricated WLED devices A-F, including CCT, Commission Internationale de l'Eclairage (CIE) coordinate, and CRI. For WLEDs based on the three phosphors with CIE color coordinates of (0.29-0.41, 0.33-0.36) in the white light region (Fig 3b), CRI values ranged from 85 to 96. These devices exhibited tunable CCT along the Planckian locus from 2805 K to 7786 K (Fig. 3b, c). Photographs of devices A-F demonstrate their gradual color change from warm white to cold white (Fig. 3c). The luminous efficiencies of WLED devices are shown in Fig. S8. The highest luminous efficiency of WLEDs is as high as 4.9 lm/W. These prototype devices need to be further optimized to improve the luminous efficiencies, including the QY of CDs and PDs, the chip efficiency, and the light-extraction efficiency through the improved device geometry.

The spectral overlap between the absorption of PFTBT PDs and the PL emission spectrum of PF10BT PDs was negligible, while there was a small spectral overlap between the absorption of PF10BT PDs and the PL emission spectrum of CDs (Fig.1d, e). Therefore, a weak energy transfer might happen between them, which would cause a shortening of the PL lifetime of CD donors and increase of the PL lifetime of PD acceptors. PL decay curves of both CD/PVP powder and mixed tri-phosphor powder were measured by TCSPC with the excitation of 405 nm and detecting wavelength of 475 nm to analyze the PL lifetime of CDs. The average PL lifetimes of CDs were almost the same, 9.3 ns and 9.2 ns for the CD/PVP powder and the mixed tri-phosphor powder, respectively (Fig. S9a). Subsequently, the PL decay curves of PF10BT/PVP, PFTBT/PVP and the mixed tri-phosphor powder probed at 540 nm and 660 nm were recorded to analyze the PL lifetimes of PF10BT and PFTBT, respectively (Fig. S9b). The PL decay time of PF10BT increased from 2.5 ns in the PF10BT/PVP powder to 5.0 ns in the mixed tri-phosphor powder, which was mainly because both CDs and PF10BT PDs contributed to the emission at 540 nm in the mixed powder (Fig. S9b). In a similar way, the PL lifetime of PFTBT PDs increased from 1.9 ns in the PFTBT/PVP powder to 2.5 ns in the mixed tri-phosphor powder. This relatively little change was due to the weak red emission of CDs. We conclude that the energy transfer between CDs and PDs was negligible in their respective powders, and their optical properties were well preserved in the fabricated WLEDs.

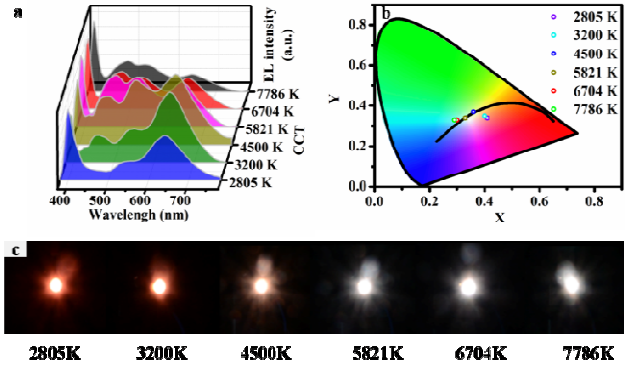

FIG. 3. (a) EL spectra of UV LED chips coated with a mixture of CD/PVP, PF10BT/PVP and PFTBT/PVP solid state phosphors with various mass ratios; **(b)** CIE color coordinates of WLED devices A-F (see Table 1 for details, the black line is the Planckian locus); **(c)** true-color photographs of WLED devices A-F.

TABLE 1. CCT, CIE coordinates (x, y), CRI and mass ratios (CD : PF10BT : PFTBT) of WLED devices A-F.

Device	CCT	CIE (x,y)	CRI	Mass ratio
A	2805 K	(0.41,0.34)	85	0.3:0.8:1.6
B	3200 K	(0.40,0.35)	88	0.7:0.8:1.7
C	4500 K	(0.36,0.36)	91	0.9:0.8:1.35
D	5821 K	(0.33,0.34)	96	1: 0.8:1.2
E	6704 K	(0.30,0.33)	91	1.3: 0.8:1
F	7789 K	(0.29,0.33)	94	1.5: 0.8:0.8

The CCT, CRI and the color coordinates of the WLED device D were recorded at different working currents to examine its optical stability. As shown in Fig. 4a, the EL bands of both CDs and PDs increased with the forward current, indicating that these solid state phosphors exhibited no saturation towards UV light. As the forward current increased from 10 to 50 mA, the color coordinates changed from (0.324, 0.344) to (0.326, 0.343) around the black body locus as shown in Fig. 4b, and they remained very close to the ideal CIE chromaticity coordinates for pure white emission (0.33, 0.33). The color coordinates of WLED shifted slightly with increased forward current, which in turn led to the slight variation of CCT from 5843 K at 10 mA to 5750 K at 50 mA, indicating its color stability. Although the UV emission intensity of the device increased faster than the phosphor's emission (Fig. 4a), it had little influence on the CCT and CRI, and the stable performance of the device was favored by little absorption between the three color phosphors.

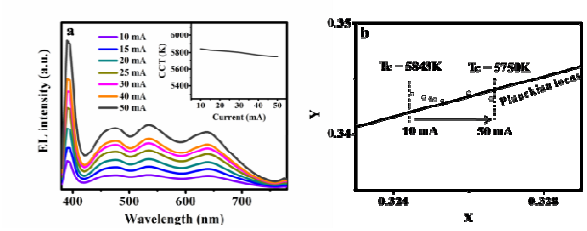

FIG. 4. (a) EL spectra of the WLED device D as a function of working current. Inset shows the corresponding CCT change; **(b)** CIE color coordinates of the WLED deviceD as a function of current from 10 to 50 mA (Tc = CCT).

In order to further evaluate the color stability of the devices, the blue, green and red monochromatic LEDs such as shown in Fig.2c were fabricated with the same amount of single-color phosphor corresponding to WLED device D, with the PVP powder replacing the omitted phosphor powder. Fig. S10 a, b and c show the emission spectra of the blue, green and red monochromatic LEDs under different working currents. The corresponding integrated intensity of each monochromatic LED versus working current is plotted in Fig. S10 d, e and f. The intensities of single-color components in the EL spectra of the WLED device D were estimated for different working currents by the Gaussian fitting, and are also presented in Fig. S10 d, e and f. The comparison indicated the similar variation of the intensities of blue, green and red color components in the WLED device as compared to the respective monochromatic LEDs. This further confirms that WLEDs based on the combination of CDs and PDs do not suffer from reabsorption effects, and show excellent color stability against the increasing current.

4.Conclusions

In summary, strongly emitting, environmentally friendly phosphors based on the blue-emitting CDs and the green- and red-emitting PDs embedded in a transparent PVP matrix were designed to prevent solid-state PL quenching between the constituting fluorophores. The FWHMs of CDs and PDs were sufficiently broad, which was beneficial for the fabrication of high CRI WLEDs. All three phosphors exhibited dominant absorption in UV spectral region, which ensured the weak reabsorption and no energy transfer crosstalk, which was beneficial to tune the resulting white emission. The WLEDs showed excellent color stability against the increasing current because the tricolor phosphors responded nearly the same to the UV variation and showed no saturation to the UV light within the wide range of working currents.

Acknowledgements

The authors appreciate the financial support from the National Natural Science Foundation of China (61106039, 51272084, 61306078, 61225018, 61475062), the National Postdoctoral Foundation (2011049015), the Jilin Province Key Fund (20140204079GX), the Hong Kong Scholar Program (XJ2012022), the State Key Laboratory on Integrated Optoelectronics (IOSKL2012ZZ12) and State Key Laboratory on Integrated Optoelectronics Fund open topics (IOSKL2014KF14), the NSF (1338346), the BORSF, and the Research Grant Council of Hong Kong S.A.R. (T23-713/11).

Notes and references

1. L.-H. Mao, W.-Q. Tang, Z.-Y. Deng, S.-S. Liu, C.-F. Wang and S. Chen, *Ind Eng Chem Res*, 2014, **53**, 6417-6425.
2. E. F. Schubert and J. K. Kim, *Science*, 2005, **308**, 1274-1278.
3. Q. Dai, C. E. Duty and M. Z. Hu, *Small*, 2010, **6**, 1577-1588.
4. S. Nizamoglu, G. Zengin and H. V. Demir, *Appl Phys Lett*, 2008, **92**, 031102.
5. H. V. Demir, S. Nizamoglu, T. Erdem, E. Mutlugun, N. Gaponik and A. Eychmüller, *Nano Today*, 2011, **6**, 632-647.
6. Y. Pan, M. Wu and Q. Su, *Mat Sci Eng B*, 2004, **106**, 251-256.
7. J. Park, M. Lim, K. Choi and C. Kim, *J Mater Sci*, 2005, **40**, 2069-2071.
8. H. S. Jang and D. Y. Jeon, *Appl Phys Lett*, 2007, **90**, 041906.
9. J. K. Park, C. H. Kim, S. H. Park, H. D. Park and S. Y. Choi, *Appl Phys Lett*, 2004, **84**, 1647-1649.
10. Q.-L. Chen, C.-F. Wang and S. Chen, *J Mater Sci*, 2013, **48**, 2352-2357.
11. J. K. Sheu, S. J. Chang, C. H. Kuo, Y. K. Su, L. W. Wu, Y. C. Lin, W. C. Lai, J. M. Tsai, G. C. Chi and R. K. Wu, *Photonics Technology Letters, IEEE*, 2003, **15**, 18-20.
12. J. X. Jiang, Y. H. Xu, W. Yang, R. Guan, Z. Q. Liu, H. Y. Zhen and Y. Cao, *Adv Mater*, 2006, **18**, 1769-1773.
13. P. I. Shih, Y. H. Tseng, F. I. Wu, A. K. Dixit and C. F. Shu, *Adv Funct Mater*, 2006, **16**, 1582-1589.
14. X. Zhang, X. Wang, J. Huang, J. Shi and M. Gong, *Opt Mater*, 2009, **32**, 75-78.
15. H. S. Chen, S. J. J. Wang, C. J. Lo and J. Y. Chi, *Appl Phys Lett*, 2005, **86**, 131905.

16. G.-Y. Lee, J. Y. Han, W. B. Im, S. H. Cheong and D. Y. Jeon, *Inorg Chem*, 2012, **51**, 10688-10694.
17. S. Nizamoglu and H. V. Demir, *Nanotechnology*, 2007, **18**, 405702.
18. X. Fang, M. Roushan, R. Zhang, J. Peng, H. Zeng and J. Li, *Chem Mater*, 2012, **24**, 1710-1717.
19. C.-H. Huang, Y.-C. Chiu, Y.-T. Yeh, T.-S. Chan and T.-M. Chen, *ACS Appl Mater Interfaces*, 2012, **4**, 6661-6668.
20. J. S. Kim, P. Jeon, J. Choi, H. Park, S. Mho and G. Kim, *Appl Phys Lett*, 2004, **84**, 2931-2933.
21. C. Sun, Y. Zhang, Y. Wang, W. Liu, S. Kalytchuk, S. V. Kershaw, T. Zhang, X. Zhang, J. Zhao, W. W. Yu and A. L. Rogach, *Appl Phys Lett*, 2014, **104**, 261106.
22. X. Wang, X. Yan, W. Li and K. Sun, *Adv Mater*, 2012, **24**, 2742-2747.
23. D. Zhou, M. Liu, M. Lin, X. Bu, X. Luo, H. Zhang and B. Yang, *ACS Nano*, 2014, **8**, 10569-10581.
24. X. Guo, C.-F. Wang, Z.-Y. Yu, L. Chen and S. Chen, *Chem Commun*, 2012, **48**, 2692-2694.
25. F. Wang, S. Pang, L. Wang, Q. Li, M. Kreiter and C.-Y. Liu, *Chem Mater*, 2010, **22**, 4528-4530.
26. S. Zhu, Q. Meng, L. Wang, J. Zhang, Y. Song, H. Jin, K. Zhang, H. Sun, H. Wang and B. Yang, *Angew. Chem.*, 2013, **125**, 4045-4049.
27. F. Wang, Z. Xie, H. Zhang, C.-Y. Liu and Y.-G. Zhang, *Adv Funct Mater*, 2011, **21**, 1027-1031.
28. K. Hola, Y. Zhang, Y. Wang, E. P. Giannelis, R. Zboril and A. L. Rogach, *Nano Today*, 2014, **9**, 590-603.
29. H. Li, Z. Kang, Y. Liu and S.-T. Lee, *J Mater Chem*, 2012, **22**, 24230-24253.
30. L. Wang, H.-Y. Wang, Y. Wang, S.-J. Zhu, Y.-L. Zhang, J.-H. Zhang, Q.-D. Chen, W. Han, H.-L. Xu, B. Yang and H.-B. Sun, *Adv Mater*, 2013, **25**, 6539-6545.
31. Y.-P. Sun, B. Zhou, Y. Lin, W. Wang, K. A. S. Fernando, P. Pathak, M. J. Meziani, B. A. Harruff, X. Wang, H. Wang, P. G. Luo, H. Yang, M. E. Kose, B. Chen, L. M. Veca and S.-Y. Xie, *J Am Chem Soc*, 2006, **128**, 7756-7757.
32. Y. Wang, S. Kalytchuk, Y. Zhang, H. Shi, S. V. Kershaw and A. L. Rogach, *J. Phys. Chem. Lett*, 2014, **5**, 1412-1420.
33. J. Chen, W. Liu, L.-H. Mao, Y.-J. Yin, C.-F. Wang and S. Chen, *J Mater Sci*, 2014, **49**, 7391-7398.
34. C.-X. Li, C. Yu, C.-F. Wang and S. Chen, *J Mater Sci*, 2013, **48**, 6307-6311.
35. W. Kwon, S. Do, J. Lee, S. Hwang, J. K. Kim and S.-W. Rhee, *Chem Mater*, 2013, **25**, 1893-1899.
36. X. Zhang, Y. Zhang, Y. Wang, S. Kalytchuk, S. V. Kershaw, Y. Wang, P. Wang, T. Zhang, Y. Zhao, H. Zhang, T. Cui, Y. Wang, J. Zhao, W. W. Yu and A. L. Rogach, *ACS Nano*, 2013, **7**, 11234-11241.
37. M. Sun, S. Qu, Z. Hao, W. Ji, P. Jing, H. Zhang, L. Zhang, J. Zhao and D. Shen, *Nanoscale*, 2014, **6**, 13076-13081.
38. Y. Wang, S. Kalytchuk, L. Wang, O. Zhovtiuk, K. Cepe, R. Zboril and A. L. Rogach, *Chem Commun*, 2015, **51**, 2950-2953.
39. Q. Hou, Q. Zhou, Y. Zhang, W. Yang, R. Yang and Y. Cao, *Macromolecules*, 2004, **37**, 6299-6305.
40. K. Chang, Z. Liu, H. Chen, L. Sheng, S. X.-A. Zhang, D. T. Chiu, S. Yin, C. Wu and W. Qin, *Small*, 2014, **10**, 4270-4275.
41. C. Wu, B. Bull, C. Szymanski, K. Christensen and J. McNeill, *ACS Nano*, 2008, **2**, 2415-2423.
42. Y. Dong, H. Pang, H. B. Yang, C. Guo, J. Shao, Y. Chi, C. M. Li and T. Yu, *Angew. Chem., Int. Ed.*, 2013, **52**, 7800-7804.